ResearchGate

See discussions, stats, and author profiles for this publication at: https://www.researchgate.net/publication/340294356

# Improved Contactless Heartbeat Estimation in FMCW Radar via Kalman Filter Tracking

**Article** *in* IEEE Sensors Letters · March 2020

DOI: 10.1109/LSENS.2020.2983706

CITATIONS
15

READS
4,622

**3 authors:**

Muhammad Arsalan
Technische Universität München
**16** PUBLICATIONS **252** CITATIONS

SEE PROFILE

Avik Santra
Infineon Technologies
**70** PUBLICATIONS **475** CITATIONS

SEE PROFILE

Christoph Will
Infineon Technologies
**18** PUBLICATIONS **349** CITATIONS

SEE PROFILE

**Some of the authors of this publication are also working on these related projects:**

Project Deep Learning for Target Recognition in Synthetic Aperture Radar (SAR) images View project

Project Novel parameter estimation algorithms for multi-user MIMO-OFDM system View project

All content following this page was uploaded by Avik Santra on 21 May 2020.

The user has requested enhancement of the downloaded file.

Sensor Applications

# Improved Contactless Heartbeat Estimation in FMCW Radar via Kalman Filter Tracking

Muhammad Arsalan, Avik Santra*, and Christoph Will**

*Infineon Technologies AG, Neubiberg, 85579, Germany*
** Senior Member, IEEE*
*** Member, IEEE*

Abstract—Radar systems enable a contactless, non-invasive method to simultaneously monitor the respiration and heart rate of a human target. To enhance the stability and accuracy of the detected heart rate, this paper introduces a Kalman filter-based tracking of the heartbeat signal. After providing a first rough estimation, the bandwidth of the applied band-pass filter is successively narrowed down and the filter limits are steadily updated with respect to the current heart rate of the target. Measurement segments with random body movements are automatically identified and consequentially ignored for the Kalman filter update. The functionality of the proposed algorithm is proven by various verification measurements using a 60-GHz frequency-modulated continuous-wave radar system. The determined heart rates are compared to the output of a commercial chest belt. Measurement data with common breathing as well as during breath-holding were recorded for fourteen different subjects.

Index Terms—Vital Sensing, FMCW Radar, Kalman Filter, Adaptive Filtering

## I. INTRODUCTION

Monitoring the vital signs of human targets finds wide usage in the fields of consumer electronics, medical care, surveillance, driver assistance, and industrial applications [1]–[3]. Radar systems enable a contactless, non-invasive method for vital sensing, which increases the comfort of the human subject and is therefore highly appreciated. This leads to a variety of applications like patient monitoring in hospitals, sleep apnea detection and presence sensing in smart homes, driver monitoring in modern cars, and physiological monitoring in surveillance and earthquake rescue operations [1], [4]–[6].

The majority of the published algorithms for radar-based vital sign measurement use the fast Fourier transform (FFT) to determine the respiration and heart rate [1], [7]–[10]. Since the FFT requires a large observation window of 10 ... 30 s, alternative approaches operating in the time domain are preferred. Furthermore, time domain-based algorithms enable the detection of individual heartbeats and are more sensitive to heart rate variability. Exemplary algorithms use feature-based correlation [11], continuous-wavelet filter and ensemble empirical mode decomposition in combination with a zero-crossing detector [12], linear demodulation to extract the heartbeat signal and subsequent autocorrelation with statistical analysis to determine the heart rate [13] or an advanced template matching algorithm investigating five heterogeneous heartbeat shapes [14]. While all listed approaches work on the filtered pulse wave signal [15], latest research utilizes detected heart sounds for heart rate calculation [16].

The aim of practical heart rate monitoring systems are to achieve high accuracy estimates while avoiding fluctuations and biases due random body movements and human motions. The algorithm proposed in this paper pursues these objectives by adaptively filtering the time domain heartbeat signal depending on the current heart rate of the subject. For the first time, the bandpass filter limits are not fixed but continuously adjust during each measurement row. The determined rate per time instance is stabilized and smoothed by applying a Kalman filter similar to [17], however we use the estimate and uncertainty further to update the bandpass filter limits. We present the functionality of the proposed algorithm using 60-GHz frequency-modulated continuous-wave (FMCW) radar chipset and prove by several measurements while comparing it to state-of-the-art algorithm with reference to a commercial chest belt.

Corresponding author: A. Santra (e-mail: avik.santra@infineon.com)
Associate Editor:
Digital Object Identifier 10.1109/LSENS.2017.0000000

## II. SIGNAL PROCESSING CHAIN

### A. FMCW Radar System Settings

FMCW radar systems, which are used to detect targets with high speed or create range-Doppler maps, commonly transmitting several frequency chirps with a short pulse repetition time (PRT) amongst them before stop chirping to save power and processing the acquired data. The number of samples per chirp defines the maximum unambiguousness range for the range FFT and depends on the chirp time as well as the sampling rate of the analog-to-digital converter (ADC). The interval between two starting times of chirp sequences is called frame time.

For pure vital sensing applications, there are different requirements to the FMCW radar system. While the PRT is not needed to be extremely short, the time interval between the last chirp of a frame to the beginning of the first chirp of the consecutive frame has to be identical to the PRT as all chirps have to be transmitted (and received) equidistantly.

### B. Pre-processing Steps

A flow chart of the required pre-processing steps is shown in Fig. 1. The target detection represents the first part, in which the range FFT is applied over all chirps of the current frame. Depending on the chosen frame time and the desired observation time, the complex FFT output is stored in a sliding window. Afterward, the amplitude of each range bin is summed up along the complete sliding window. The peak in this output signal within the chosen minimum and maximum ranges defines the target range bin of the current update [10]. Nevertheless, data is only further processed if the standard deviation in this range

bin along the sliding window is above a predefined threshold, which is depicted as movement detection.

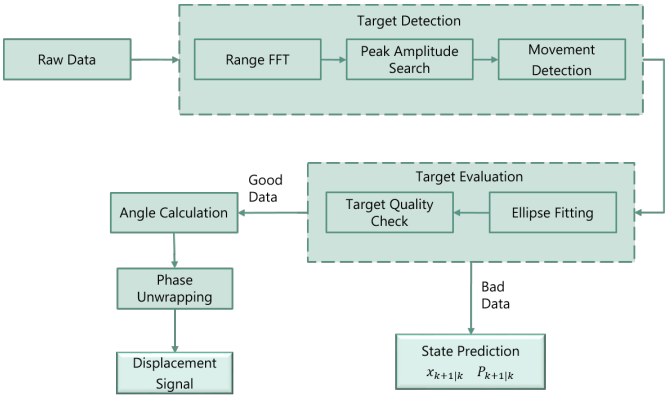


Fig. 1. Flow chart of the pre-processing steps.

In the second part, the quality of the complex target data is evaluated. After applying an ellipse fitting algorithm similar to [18] to compensate for offset, amplitude, and gain errors, the deviation of the reconstructed circle from the ideal unit circle is calculated. Only if the deviation is below a certain threshold, the heart rate estimation and state in Kalman filter are updated. This prevents that low quality data inflicted by random body movements erroneously change the passband settings and thus corrupt the heart rate estimation. In case of low quality data only the state prediction of Kalman filter is applied. Exemplary in-phase (I) and quadrature (Q) plots of (a) low and (b) high quality compensated target data are depicted in Fig. 2.

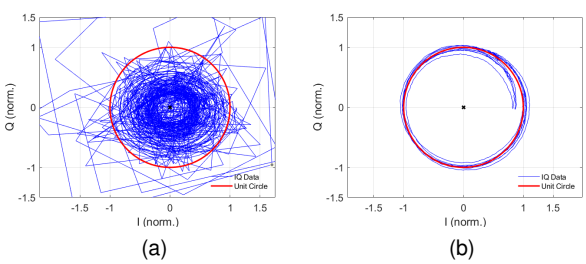


Fig. 2. Exemplary IQ plots of (a) low and (b) high quality target data.

The angle of the compensated target data is calculated by arctangent demodulation and the resulting phase values in the range of $[-\pi,+\pi)$ are unwrapped between two consecutive data points. This phase is unwrapped by adding or subtracting $2\pi$ for phase jumps larger than $-\pi$ or $+\pi$, respectively. With $\lambda$ being the wavelength of the carrier frequency and $\lambda/2$ representing the unambiguousness (phase) range, the displacement of the target can subsequently be calculated by the following formula:

$$\Delta d = \frac{\lambda}{4\pi} \cdot \text{unwrap}\left(\arctan\frac{Q}{I}\right). \tag{1}$$

## C. Adaptive Heartbeat Filtering and Heart Rate Tracking

A flow chart of the main part of the proposed algorithm is shown in Fig. 3. In the first step of the signal processing loop, the displacement signal as the output of the pre-processing steps is bandpass filtered with a fourth-order Butterworth filter to extract the heartbeat signal. A peak search considering a minimum peak prominence is applied to detect the individual heartbeats, which are subsequently used to calculate a new temporary heart rate value. Initially, the passband range is set to 0.7 ... 3.0 Hz, which corresponds to a heart rate of 42 ... 180 bpm (beats per minute). If new high quality target data have been acquired in a frame, the filter limits are adjusted depending on the previously and currently detected heart rates, else the passband range stays the same. In principle, the aim is to narrow down the passband range, to suppress the higher frequency components of the pulse wave in the heartbeat signal [15], which arise due to higher amplitude components of the harmonics from respiration. In case of high quality target data, the filter settings are updated after state prediction and a gating procedure of the Kalman filter. The functionality of these signal processing steps is explained in the following paragraph.

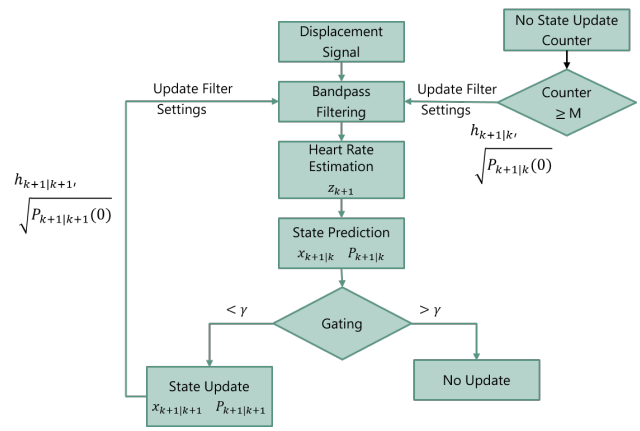


Fig. 3. Flow chart of the main part of the proposed algorithm.

Kalman filtering is a recursive Bayesian process, which is applied, when the measured values contain unpredictable or random errors, uncertainties or variations. The state vector is expressed as

$$x = \begin{bmatrix} h & \dot{h} & \ddot{h} \end{bmatrix}^T \tag{2}$$

where $h, \dot{h}, \ddot{h}$ represents the heart rate in Hz, its first order derivative, and second-order derivative resp. The state vector in Kalman filter at frame time $k$ is represented as Gaussian process with mean $x_{k|k}$ and covariance or uncertainty $P_{k|k}$.

In the proposed algorithm, the Kalman filter is designed as constant acceleration model, thus the state transition model predicting the state in frame $k+1$ from state vector in frame $k$ is given as

$$x_{k+1|k} = Ax_{k|k} = \begin{bmatrix} 1 & \Delta t & 0.5\Delta t^2 \\ 0 & 1 & \Delta t \\ 0 & 0 & 1 \end{bmatrix} x_{k|k} \tag{3}$$

in which $\Delta t$ denotes the time elapsed between two frames. The observation model is provided as

$$y_{k+1} = Hx_{k+1|k} = \begin{bmatrix} 1 & 0 & 0 \end{bmatrix} x_{k+1|k} \tag{4}$$

The measured heart rate estimation value from the peak count algorithm is denoted as $z_{k+1}$. The uncertainty of the state prediction originates from process noise and is modeled as $Q = GG^T\rho_a^2$, where $G$ is $[0.5\Delta t^2 \quad \Delta t \quad 1]$ and $\rho_a^2$ represents the acceleration process noise. The variance of the measurement noise is denoted as $R = \delta h^2$, which represents the expected square of the estimation error.

Once the first vital data is recorded a track is initialized with default $Q$, $R$ noise matrices and initial state and covariance $x_{0|0}, P_{0|0}$ along with default filter settings, the proposed algorithm operates at each frame k as follows

1) Bandpass Filtering: The pre-processed displacement signal is band-pass filter whose cutoff frequencies are defined by the state update from earlier frame
2) Peak Count Estimation: The heart rate estimation $z_{k+1}$ is obtained in time-domain through peak counts
3) State Prediction

$$\begin{aligned} x_{k+1|k} &= Ax_{k|k} \\ P_{k+1|k} &= AP_{k|k}A^T + Q \end{aligned} \tag{5}$$

4) Ellipsoidal Gating

$$\begin{aligned} y_{k+1} &= Hx_{k+1|k} \\ (z_{k+1} - y_{k+1})^T P_{k+1|k}^{-1}(z_{k+1} - y_{k+1}) &\lesseqgtr \gamma \end{aligned} \tag{6}$$

The ellipsoidal gating function checks if the heart rate estimate $z_{k+1}$ is within the gating window if its outside the ellipsoidal window then no Kalman filter update is done as the estimated data is an outlier. If its within the window the Kalman filter is updated

5) State Update

$$\begin{aligned} K_{k+1} &= P_{k+1|k}H^T(HP_{k+1|k}H^T + R)^{-1} \\ x_{k+1|k+1} &= x_{k+1|k} + K_{k+1}(z_{k+1} - y_{k+1}) \\ P_{k+1|k+1} &= (I - K_kH)P_{k+1|k} \end{aligned} \tag{7}$$

6) Update Filter Settings: Based on the updated state, the bandpass filter settings are updated as $h_{k+1|k+1} - \sqrt{P_{k+1|k+1}(1,1)}, h_{k+1|k+1} + \sqrt{P_{k+1|k+1}(1,1)}$

In case, the Kalman Filter state update is not done for $M$ consecutive frames either because of low quality data (large deviation from unit circle) or estimation outside gating window then the filter settings are updated using the state prediction as $(h_{k+1|k} - \sqrt{P_{k+1|k}(1,1)}, h_{k+1|k} + \sqrt{P_{k+1|k}(1,1)})$. This helps in translating the center frequency and also increasing the bandpass filter cutoff settings to account for the fact that we the true heart rate might have drifted during the period there were no updates. The track is killed and filter settings reset once there is no target detections for $N$ consecutive frames.

## III. EXPERIMENTAL RESULTS

In the verification measurements, the FMCW radar chip *BGT60TR13C* from *Infineon Technologies AG* in Fig. 4a was used. The frequency chirps used a bandwidth of 2.0 GHz within the 60-GHz band, where the smaller wavelength helps with the phase accuracy. The PRT was set to 5 ms, which corresponds to an effective sampling rate of 200 Hz. A frame time of 1.28 s was chosen, as well as an observation window of eight frames (~10 s). The ADC to digitize the data has a resolution of 12 bit and the data was sent from the evaluation board via USB to the PC working as master. Measurement data were gathered, processed, and evaluated in *MATLAB*.

The subjects were placed in front of the radar at a distance of approximately 40 cm as depicted in Fig. 4b without any supervised restriction on random-body movements performed. The commercial chest belt *Polar H7* was used as heart rate reference sensor. Fourteen human healthy subjects (10 male, 4 female, BMI: 22.0 ± 3.2) participated in the experimental results. For half of the subjects, measurement row with common breathing and for another half measurement row with breath-holding was recorded. All measurement rows have a length of 16 frames, which corresponds to approximately 20 s.

(a) (b)

Fig. 4. (a) *Infineon BGT60TR13C* radar system and (b) experimental setup.

The data of each measurement row was first completely acquired and afterward evaluated. The frame time was artificially changed to one second and the length of the sliding window was set to 10 s, which results in eleven heart rate values per measurement row. The performance of the proposed algorithm in comparison to spectral analysis-based algorithm [9] is evaluated in Fig. 5, in which each line represents one measurement row. We chose this algorithm for comparison as the base signal processing blocks are similar to the proposed algorithm. The blue lines depict the reference values, while the red lines represent the output of the pure peak detection based on spectral-analysis with fixed (initial) passband settings and the green lines depict the results of the proposed algorithm.

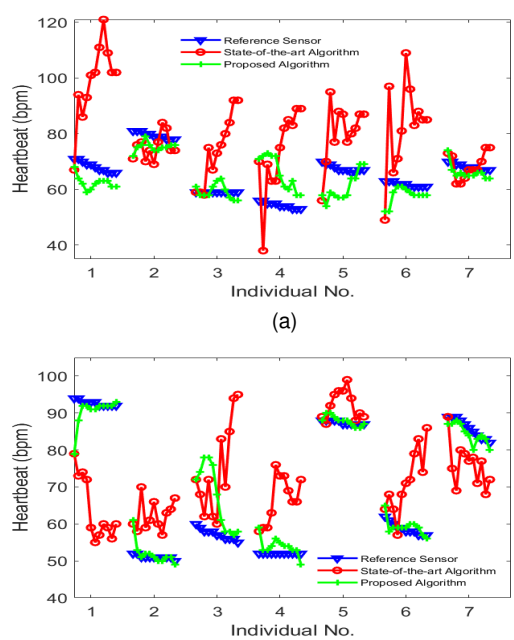


Fig. 5. Experimental results (a) during breath-holding and (b) with common breathing among different indiviuals comparing proposed algorithm to spectral analysis-based algorithm.

The proposed algorithm achieves better results than the state-of-art spectral analysis-based algorithm in all measurement rows,

as illustrated in Fig. 5a. The heart rate values for fixed passband settings show a high deviation from the reference sensor and sometime have large jumps between two consecutive values. Even small body movements can cause large jumps in the heartbeat signal estimation if extracted with a broad passband. Narrowing down the bandwidth and tracking the heart rate value prevents such jumps and smooths the estimated values. While the first values sometimes show a considerable deviation, the Kalman filtering approximates the value towards the reference value step by step. The resulting root-mean-square errors (RMSE) for proposed algorithm are 5.3 bpm and 7.0 bpm compared to 17.6 bpm and 21.3 bpm obtained with state-of-the-art algorithm for common breathing and breath-holding cases, respectively. The proposed algorithm outperforms the state-of-the-art method by a factor of three in terms of RMSE at the cost of 1.1 times compute time. The bad performance in some measurement rows especially for the state-of-the-art algorithm is the influence of harmonics of the breathing signal, intermodulations with the breathing signal or higher frequency pulse wave components in the heartbeat signal extracted with a broad passband.

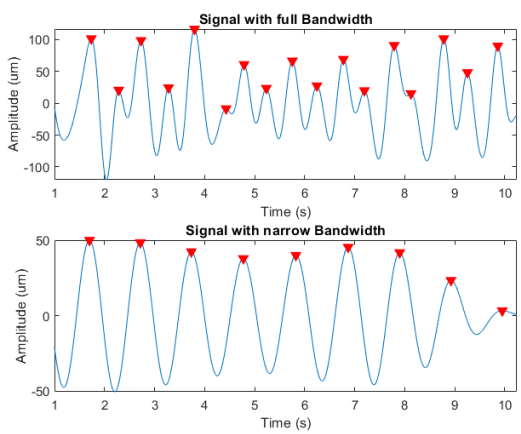


Fig. 6. Effect of narrowing down the bandwidth.

The effect of narrowing down the passband bandwidth is illustrated in Fig. 6. During the shown time window, the human subject had a heart rate of 59 bpm. In the upper sub-plot, the filter limits are set to the initial settings, which leads to too many detected peaks and therefore a too high heart rate of 117 bpm. With the narrowing down the heart rate to the minimum passband range of 0.3 Hz, one peak per heartbeat is detected and therefore a quite accurate heart rate of 58 bpm is estimated. If the first estimates with larger bandwidth are wrong, the Kalman filter approximates to a different frequency component, which explains the moderate results of some measurement rows.

## IV. CONCLUSION

This paper presented a novel algorithm for heart rate estimation with (FMCW) radar system utilizing an adaptive bandpass filter to extract the heart rate signal along with Kalman filter-based tracking procedure. The combination of these steps leads to narrowing of the passband range while simultaneously approximating the actual heart rate as center frequency. The output values are shown to outperform state-of-the-art radar-based method in reference to a chest sensor.

## REFERENCES

[1] C. Li, V. M. Lubecke, O. Boric-Lubecke, and J. Lin, "A review on recent advances in doppler radar sensors for noncontact healthcare monitoring," *IEEE Transactions on Microwave Theory and Techniques*, vol. 61, no. 5, pp. 2046–2060, May 2013.

[2] C. Li, Z. Peng, T. Huang, T. Fan, F. Wang, T. Horng, J. Munoz-Ferreras, R. Gomez-Garcia, L. Ran, and J. Lin, "A review on recent progress of portable short-range noncontact microwave radar systems," *IEEE Transactions on Microwave Theory and Techniques*, vol. 65, no. 5, pp. 1692–1706, May 2017.

[3] Z. Peng, J. M. Munoz-Ferreras, Y. Tang, C. Liu, R. Gomez-Garcia, L. Ran, and C. Li, "A portable fmcw interferometry radar with programmable low-if architecture for localization, isar imaging, and vital sign tracking," *IEEE Transactions on Microwave Theory and Techniques*, vol. 65, no. 4, pp. 1334–1344, April 2017.

[4] C. Li, J. Lin, and Y. Xiao, "Robust overnight monitoring of human vital signs by a non-contact respiration and heartbeat detector," in *2006 International Conference of the IEEE Engineering in Medicine and Biology Society*, Aug 2006, pp. 2235–2238.

[5] C. Gu, "Short-range noncontact sensors for healthcare and other emerging applications: A review," *Sensors*, vol. 16, no. 8, p. 1169, 2016.

[6] K. Van Loon, M. Breteler, L. Van Wolfwinkel, A. R. Leyssius, S. Kossen, C. Kalkman, B. van Zaane, and L. Peelen, "Wireless non-invasive continuous respiratory monitoring with fmcw radar: a clinical validation study," *Journal of clinical monitoring and computing*, vol. 30, no. 6, pp. 797–805, 2016.

[7] Y. Xiong, S. Chen, X. Dong, Z. Peng, and W. Zhang, "Accurate measurement in doppler radar vital sign detection based on parameterized demodulation," *IEEE Transactions on Microwave Theory and Techniques*, vol. PP, no. 99, pp. 1–10, 2017.

[8] L. Chioukh, H. Boutayeb, D. Deslandes, and K. Wu, "Noise and sensitivity of harmonic radar architecture for remote sensing and detection of vital signs," *IEEE Transactions on Microwave Theory and Techniques*, vol. 62, no. 9, pp. 1847–1855, Sept 2014.

[9] A. Santra, R. V. Ulaganathan, T. Finke, A. Baheti, D. Noppeney, J. R. Wolfgang, and S. Trotta, "Short-range multi-mode continuous-wave radar for vital sign measurement and imaging," in *2018 IEEE Radar Conference (RadarConf18)*, April 2018, pp. 0946–0950.

[10] M. Alizadeh, G. Shaker, J. C. M. De Almeida, P. P. Morita, and S. Safavi-Naeini, "Remote monitoring of human vital signs using mm-wave fmcw radar," *IEEE Access*, vol. 7, pp. 54 958–54 968, 2019.

[11] T. Sakamoto, R. Imasaka, H. Taki, T. Sato, M. Yoshioka, K. Inoue, T. Fukuda, and H. Sakai, "Feature-based correlation and topological similarity for interbeat interval estimation using ultrawideband radar," *IEEE Transactions on Biomedical Engineering*, vol. 63, no. 4, pp. 747–757, 4 2016.

[12] W. Hu, Z. Zhao, Y. Wang, H. Zhang, and F. Lin, "Noncontact accurate measurement of cardiopulmonary activity using a compact quadrature doppler radar sensor," *IEEE Transactions on Biomedical Engineering*, vol. 61, no. 3, pp. 725–735, March 2014.

[13] W. Massagram, V. M. Lubecke, A. Host-Madsen, and O. Boric-Lubecke, "Assessment of heart rate variability and respiratory sinus arrhythmia via doppler radar," *IEEE Transactions on Microwave Theory and Techniques*, vol. 57, no. 10, pp. 2542–2549, Oct 2009.

[14] C. Will, K. Shi, R. Weigel, and A. Koelpin, "Advanced template matching algorithm for instantaneous heartbeat detection using continuous wave radar systems," in *2017 First IEEE MTT-S International Microwave Bio Conference (IMBIOC)*, May 2017, pp. 1–4.

[15] C. Will, K. Shi, S. Schellenberger, T. Steigleder, F. Michler, R. Weigel, C. Ostgathe, and A. Koelpin, "Local pulse wave detection using continuous wave radar systems," *IEEE Journal of Electromagnetics, RF and Microwaves in Medicine and Biology*, vol. PP, no. 99, pp. 1–1, 2017.

[16] C. Will, K. Shi, S. Schellenberger, T. Steigleder, F. Michler, J. Fuchs, R. Weigel, C. Ostgathe, and A. Koelpin, "Radar-based heart sound detection," *Scientific reports*, vol. 8, no. 1, p. 11551, 2018.

[17] M. S. Rahman, M. M. Haque, B.-J. Jang, and K.-D. Kim, "Extended kalman filter for doppler radar cardiopulmonary monitoring system," in *2012 7th International Conference on Electrical and Computer Engineering*. IEEE, 2012, pp. 264–267.

[18] A. Singh, X. Gao, E. Yavari, M. Zakrzewski, X. H. Cao, V. M. Lubecke, and O. Boric-Lubecke, "Data-based quadrature imbalance compensation for a cw doppler radar system," *IEEE Transactions on Microwave Theory and Techniques*, vol. 61, no. 4, pp. 1718–1724, April 2013.

View publication stats